# Segmentation of Dual-Axis Swallowing Accelerometry Signals in Healthy Subjects With Analysis of Anthropometric Effects on Duration of Swallowing Activities

Ervin Sejdić*, *Member, IEEE*, Catriona M. Steele, and Tom Chau, *Senior Member, IEEE*

***Abstract*—Dysphagia (swallowing difficulty) is a serious and debilitating condition that often accompanies stroke, acquired brain injury, and neurodegenerative illnesses. Individuals with dysphagia are prone to aspiration (the entry of foreign material into the airway), which directly increases the risk of serious respiratory consequences such as pneumonia. Swallowing accelerometry is a promising noninvasive tool for the detection of aspiration and the evaluation of swallowing. In this paper, dual-axis accelerometry was implemented since the motion of the hyolaryngeal complex occurs in both anterior–posterior and superior–inferior directions during swallowing. Dual-axis cervical accelerometry signals were acquired from 408 healthy subjects during dry, wet, and wet chin tuck swallowing tasks. The proposed segmentation algorithm is based on the idea of sequential fuzzy partitioning of the signal and is well suited for long signals with nonstationary variance. The algorithm was validated with simulated signals with known swallowing locations and a subset of 295 real swallows manually segmented by an experienced speech language pathologist. In both cases, the algorithm extracted individual swallows with over 90% accuracy. The time duration analysis was carried out with respect to gender, body mass index (BMI), and age. Demographic and anthropometric variables influenced the duration of these segmented signals. Male participants exhibited longer swallows than female participants ($p = 0.05$). Older participants and participants with higher BMIs exhibited swallows with significantly longer ($p = 0.05$) duration than younger participants and those with lower BMIs, respectively.**

***Index Terms*—Accelerometry, dysphagia, segmentation, time duration analysis.**

## I. Introduction

THE MEASUREMENT of neck vibrations associated with deglutition is known as swallowing accelerometry, a potentially informative adjunct to bedside screening for dysphagia [1]–[6]. Accelerometric measurements are minimally invasive, requiring only the superficial attachment of a sensor anterior to the thyroid notch. There has been an interest in exploiting this vibration signal for dysphagia screening. Combining accelerometry and swallow pressure, Suryanarayanana *et al.* [7] developed a hand-crafted fuzzy rule base to classify 16 patients with dysphagia according to aspiration risk. From a physiological perspective, Reddy *et al.* [4] attributed the accelerometric signal to the extent of laryngeal elevation during swallowing, thus arguing that accelerometry would be of diagnostic value. On this premise, Das *et al.* [5] proposed a hybrid fuzzy logic committee of neural networks trained to accurately distinguish between swallows from a dozen healthy subjects and 16 with dysphagia. In a pediatric study involving children with dysphagia secondary to cerebral palsy, swallow accelerometry signals were found to be largely nonstationary [8], while an offline radial basis classifier using two time-domain features differentiated between manually segmented aspiration events and safe swallows with 80% sensitivity and specificity [6].

A critical first step in the systematic analysis of swallowing accelerometry signals is the demarcation of individual swallows within an extended recording of vibrations collected from the neck. Previous studies have only investigated a small number of swallows, and hence, data were conducive to manual segmentation by a human analyst. Larger volumes of accelerometry data necessitate an automatic method to mitigate human error due to fatigue or oversight and to ensure consistent segmentation criteria. Segmentation algorithms have been developed in other fields, e.g., heart sounds analysis [9], speech analysis [10], electroencephalogram signals analysis [11], knee joint vibroarthrographic signals analysis [12], and in the analysis of uterine magnetomyogram contractions during pregnancy [13], to name a few. In particular, several successful methods rely on multiple channels of information to enhance segmentation [14], [15]. In swallow accelerometry, we can exploit both anterior–posterior (A-P) and superior–inferior (S-I) vibrations for this purpose. In addition, there appears to be a physiological basis for considering dual-axis accelerometry, given the 2-D movement of the hyoid and larynx during swallowing [16], [17].

The contributions of this paper are twofold. First, this paper introduces a systematic algorithm for the segmentation of dual-axis swallowing accelerometry signals, a problem that has not been previously addressed in the literature. The proposed segmentation algorithm considers the stochastic properties of swallowing signals in both directions, A-P and S-I, successfully

Manuscript received June 19, 2008; revised September 15, 2008. First published January 20, 2009; current version published May 6, 2009. This work was supported in part by the Ontario Centres of Excellence, by the Toronto Rehabilitation Institute, by the Bloorview Kids Rehab, and by the Canada Research Chairs Program. *Asterisk indicates corresponding author.*

*E. Sejdić is with the Bloorview Research Institute and the Institute of Biomaterials and Biomedical Engineering, University of Toronto, Toronto, ON M4G 1R8, Canada (e-mail: esejdic@ieee.org).

C. M. Steele is with the Toronto Rehabilitation Institute and the Department of Speech-Language Pathology, University of Toronto, Toronto, ON M4G 1R8, Canada (e-mail: steele.catriona@torontorehab.on.ca).

T. Chau is with the Bloorview Research Institute and the Institute of Biomaterials and Biomedical Engineering, University of Toronto, Toronto, ON M4G 1R8, Canada (e-mail: tom.chau@utoronto.ca).

Digital Object Identifier 10.1109/TBME.2008.2010504

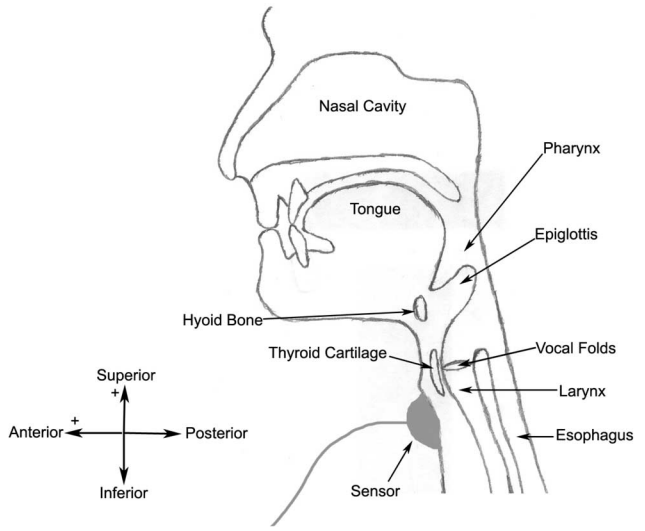


Fig. 1. Location and orientation of the sensor (shaded oval) on a participant's neck.

extracting events associated with swallowing in over 90% of all cases considered. Second, this paper presents the analysis of the time duration of swallows with respect to gender, body mass index (BMI), and age for 408 healthy subjects. In order to eventually recognize differences between normal and dysphagic swallowing, the healthy, nondysphagic swallow must first be rigorously studied [18]. In addition, three types of swallows are considered, namely, saliva swallows, water swallows in a neutral position, and water swallows in a chin tuck position. These types of swallows are typically considered during swallowing assessment [19].

The paper is organized as follows. Section II outlines the experimental approach and data acquisition procedures. In Section III, segmentation is considered in detail and an algorithm for dual-axis swallowing accelerometry signals is proposed. Section IV discusses the results of segmentation and time duration analysis.

## II. Methodology

In all, 408 participants (aged 18–65) were recruited over a three-month period from a public science center. All participants provided written consent. The study protocol was approved by the research ethics boards of the Toronto Rehabilitation Institute and the Bloorview Kids Rehab, both located in Toronto, ON, Canada. Participants had no documented swallowing disorders and passed an oral mechanism exam prior to participation.

Participants sat behind a screen for privacy. They answered a set of questions relating to medical and swallowing history. A speech language pathologist (SLP) measured the height, weight, body fat percentage (BIA Meter, BC-550, Tanita), and mandibular jaw length of each participant. A dual-axis accelerometer (ADXL322, Analog Devices) was attached to the participant's neck (anterior to the cricoid cartilage) using double-sided tape. The axes of acceleration were aligned to the A-P and S-I directions, as shown in Fig. 1. Data were bandpass-filtered in hardware with a passband of 0.1–3000 Hz and sampled at 10 kHz using a custom LabVIEW program running on a laptop. Data were saved for subsequent offline analysis.

With the accelerometer attached, each participant was cued to perform five saliva swallows. After each swallow, there was a brief rest to allow for saliva production. Subsequently, the participant completed five water swallows by cup with their chin in the natural position (i.e., perpendicular to the floor) and five water swallows in the chin-tucked position. Water was served chilled in ten individual cups so that pre- and postswallow cup weight could be measured on a digital scale. These measurements facilitated the estimation of bolus volume. Previous research suggested that natural sip size during this kind of task is between 5 and 8 mL per sip [20]. The entire data collection session lasted 15 min per participant.

Examination of the collected data revealed that some acquired signals were inadequate for further analysis due to the presence of strong disturbances, such as vocalizations, coughing, and excessive head movements. Nevertheless, 9800 swallows were retained for subsequent analysis.

## III. Segmentation of Dual-Axis Accelerometry Signals

Often signals can be considered to have segments with different stochastic behavior such that a realization of a process given by $N$ points, $\{x_i | 1 \leq i \leq N\}$, can be composed of $K$ segments with $K-1$ transition times $\tau = \{t_1, t_2, \ldots, t_{K-1}\}$, where $t_k \in \mathbb{Z}^+$. Furthermore, the data within the $k$th segment can be assumed to follow an independent and identically distributed Gaussian distribution with variance $\sigma_k^2$. Hence, the probability density function (pdf) for data within the $k$th segment would be given by

$$\ln p(x_{t_{k-1}}, \ldots, x_{t_k-1} \,|\sigma_k^2) = -\frac{t_k - t_{k-1}}{2} \ln\left(2\pi\sigma_k^2\right) - \frac{\sum_{i=t_{k-1}}^{t_k-1} x_i}{2\sigma_k^2}. \quad (1)$$

By writing $\theta_K = \{\sigma_1^2, \sigma_2^2, \ldots, \sigma_k^2\}$, which indicates the vector of variances for all $K$ segments, and assuming that these segments are statistically independent, the pdf of the dataset $\{x\}$ can be written as

$$p(x \,|\tau, \theta_K, K) = \prod_{k=1}^{K} p(x_{t_{k-1}}, \ldots, x_{t_k-1} \,|\sigma_k^2) \quad (2)$$

where, by definition, $t_0 \equiv 0$ and $t_{k-1} \equiv N$. Then, the segmentation problem demands a joint estimation of $\tau, \theta_K$, and $K$. The determined values would represent the best fit of the data $x$ to (2). Different solutions to this segmentation problem have been proposed in the literature over the years [21]–[23]. However, computational costs associated with the proposed solutions are very high. Recently, a very simple algorithm that determines the number of segments automatically and avoids threshold tuning was proposed by Wang and Willett [24].

### A. Minimum Description Length (MDL) Based Sequential Segmentation

Wang and Willett's algorithm begins with an initial assumption that the length of any segment is bounded below by $L_{\min}$ and above by $L_{\max}$

$$L_{\min} \leq t_k - t_{k-1} \leq L_{\max}. \tag{3}$$

This assumption mandates that there is at most one change during any interval of length $L_{\min}$. In other words, for $\{x_i | t_{k-1} \leq i \leq t_k + L_{\min} - 1\}$, only two situations are possible, and they are given by the following hypotheses.

*Hypothesis 1:* $x_i \sim N(0, \sigma_k^2)$, for $t_{k-1} \leq i \leq t_k + L_{\min} - 1$.

*Hypothesis 2:* $\exists l_o \in [L_{\min}, L_{\max}]$, such that $x_i \sim N(0, \sigma_k^2)$ for $t_{k-1} \leq i \leq l_o$ and $x_i \sim N(0, \sigma_{k+1}^2)$ for $l_o + 1 \leq i \leq t_k + L_{\min} - 1$.

Here, $\sigma_k^2$ and $\sigma_{k+1}^2$ are distinguishable. In other words, the segment is either homo- or heteroscedastic. The value of $l_o$ is estimated through the following relation [24]:

$$\begin{aligned}\widehat{l}_o = \arg \max_{l_o \in [L_{\min}, L_{\max}]} \Bigg\{ & -\frac{l_o - t_{k-1}}{2} \ln(2\pi \widehat{\sigma}_k^2) - \frac{\sum_{i=t_{k-1}}^{l_o} x_i^2}{2\widehat{\sigma}_k^2} \\ & - \frac{t_k + L_{\min} - 1 - (l_o + 1)}{2} \ln\left(2\pi \widehat{\sigma}_{k+1}^2\right) \\ & - \frac{\sum_{i=l_o+1}^{t_k + L_{\min} - 1} x_i^2}{2\widehat{\sigma}_{k+1}^2} \Bigg\}\end{aligned} \tag{4}$$

where

$$\widehat{\sigma}_k^2 = \frac{1}{l_o - t_{k-1} - 1} \sum_{i=t_{k-1}}^{l_o} x_i^2 \tag{5}$$

$$\widehat{\sigma}_{k+1}^2 = \frac{1}{L_{\min}} \sum_{i=l_o+1}^{l_o + L_{\min}} x_i^2. \tag{6}$$

The data contained in the segment given $\chi = \{x_i | t_{k-1} \leq i \leq \widehat{l}_o + L_{\min} - 1\}$ satisfies either case 1 or case 2. In order to determine which hypothesis best describes the segment $\chi$, the MDL principle is employed as follows [24]:

$$\begin{aligned}\widehat{c} &= \arg \max_{c \in [1,2]} \text{MDL}(c; \chi) \\ &= \arg \max_{c \in [1,2]} I_c(N_\chi) - \frac{2c - 1}{2} \ln(N_\chi)\end{aligned} \tag{7}$$

where $N_\chi$ is the length of $\chi$, and

$$\begin{aligned}I_c(N_\chi) = & \max_{\{T_1, T_2, \ldots, T_{l-1}\} \in [L_{\min}, L_{\max}], T_0 = 1, T_l = N_\chi} \\ & \times \sum_{i=1}^{c} -\frac{T_i - T_{i-1}}{2} \left(\ln\left(2\pi \widehat{\sigma}_i^2\right) + 1\right)\end{aligned} \tag{8}$$

with $\widehat{\sigma}_i^2$ being the maximum likelihood (ML) estimate of variance for time interval $T \in [T_{i-1}, T_i]$.

Based on the value produced by (7), a decision is reached for the given segment. This procedure continues until the entire signal is analyzed. Wang and Willett also proposed a *post hoc* refinement stage to improve the accuracy of segmentation. For full details about the algorithm and its implementation, refer to [24].

For simulated Gaussian time series with zero mean and piecewise constant variance, and lengths up to 6000 points, the algorithm reportedly performs accurately, with computation times comparable to, if not shorter than, those of competing algorithms [24]. However, for the swallowing records considered in this paper, which are of considerable length ($\gg 10^4$ points), the approximately linear complexity of the algorithm results in a marked increase in computational time. This computation cost is further heightened when considering the two realizations of the same process (i.e., dual-axis swallowing accelerometry). Swallowing accelerometry signals often possess nonstationary variance [8], and hence, the present algorithm may "overestimate" the number of segments. For example, a slight change in variance within the boundaries of a given segment would cause the algorithm to detect a transition point, when, in fact, the segment may be a single, cohesive swallowing event from the physiological point of view. Hence, for the present application, it is necessary to detect distinct physiological events (i.e., swallowing versus nonswallowing activity), rather than small fluctuations in variance. In the next section, a modified version of the Wang and Willet's algorithm is proposed to deal with the aforementioned challenges of lengthy dual-axis swallowing accelerometry signals.

### B. Proposed Sequential Segmentation

The computational bottleneck of Wang and Willet's algorithm lies in the optimization procedures to estimate the transition point $l_0$ and the segment class $\hat{c}$. To reduce the computational load, one may exploit characteristics of the problem at hand to simplify the optimization procedures. First, exact locations of the onsets and offsets of swallows are unknown and can only be approximately determined. Hence, forcing the algorithm to determine the optimal value for $l_0$, i.e., the exact locations of onsets and offsets, is unnecessary in the swallowing application. Second, the present goal of segmentation is not to detect small changes in variances, but rather large changes. In light of the above, we propose the following two modified hypotheses for sequential segmentation.

*Hypothesis 1:* $\phi_i \sim g_1(\phi|\theta_1)$, for $t_{k-1} \leq i \leq t_{k-1}$.
*Hypothesis 2:* $\phi_i \sim g_2(\phi|\theta_2)$, for $t_{k-1} \leq i \leq t_{k-1}$.

Here, $\phi$ is a variable related to $x$, $g_1(\phi|\theta_1)$ and $g_2(\phi|\theta_2)$ are conditional pdfs, and $\theta_1$ and $\theta_2$ are unknown parameter vectors. The pdf $g_1(\phi|\theta_1)$ represents the absence of swallowing activity, while $g_2(\phi|\theta_2)$ models the presence of swallowing activity. Before discussing the detection procedure, we first examine the formulation of a variable $\phi$, which is related to $x$.

Due to the fact that datasets are very long and the swallowing signals are buried in contaminating noise-like signals likely arising from both instrumentation and physiological sources, the relationship between $\phi$ and $x$ is to be formed in a piecewise and stochastic manner. To follow Wang and Willett's algorithm, it is assumed that $\phi$ is a piecewise constant estimate of the variance of $x$, i.e., choose $L \in \mathbb{Z}^+$ satisfying relation (3) and

$M > L, M \in \mathbb{Z}^+$. Furthermore, it is assumed that $L < M$ in order to have $M - L$ overlaps in sequential procedure. To relate the entire signal $x$ to the variable $\phi$, the following steps are proposed.

1) Initialize $\nu_k = 1$ and set $\mathbf{y} = \{x_i | \nu_k \leq i \leq \nu_k + M - 1\}$.
2) Estimate the sample mean of $\mathbf{y}$

$$\widehat{\mu}_y = E\{\mathbf{y}\} \approx \frac{1}{M} \sum_{i=1}^{M} y_i. \tag{9}$$

3) Estimate the sample standard deviation of $\mathbf{y}$ in an ML sense

$$\widehat{\sigma}_y = \sqrt{\frac{1}{M} \sum_{i=1}^{M} (y_i - \widehat{\mu}_y)^2}. \tag{10}$$

4) Set the variable $\boldsymbol{\phi}$ as follows:

$$\phi_i = \widehat{\sigma}_y, \qquad \text{for } \nu_k \leq i \leq \nu_k + M - 1. \tag{11}$$

5) Set $\nu_{k+1} = \nu_k + L$ and proceed to step 2 until the entire signal is analyzed.

It can be assumed that the vector $\boldsymbol{\phi}$ of standard deviations is sampled from $g_1(\boldsymbol{\phi}|\theta_1)$ and $g_2(\boldsymbol{\phi}|\theta_2)$ with *a priori* probabilities $P_1$ and $P_2$, respectively, where $0 < P_1, P_2 < 1$, and $P_1 + P_2 = 1$. However, since these *a priori* probabilities are not known, it has to be assumed that $\boldsymbol{\phi}$ is sampled from $p(\boldsymbol{\phi}|\xi)$, which is a pdf representing a mixture of $g_1(\boldsymbol{\phi}|\theta_1)$ and $g_2(\boldsymbol{\phi}|\theta_2)$, with mixing parameters being $P_1$ and $P_2$. In other words, $p(\boldsymbol{\phi}|\xi)$ is given by

$$p(\boldsymbol{\phi}\,|\xi) = P_1 g_1(\boldsymbol{\phi}\,|\theta_1) + P_2 g_2(\boldsymbol{\phi}\,|\theta_2) \tag{12}$$

where $\xi = \{P_1, P_2, \theta_1, \theta_2\}$. Therefore, the mixture separation problem boils down to the estimation of the members of $\xi$. Let the set $\Phi$ drawn from $p(\boldsymbol{\phi}|\xi)$ represent all possible outcomes of independent trials, then the ML estimate of $\xi$ would be given by

$$\xi^* = \arg\max_{\xi} \sum_{\boldsymbol{\phi} \in \Phi} \ln p(\boldsymbol{\phi}\,|\xi). \tag{13}$$

Nevertheless, finding the ML estimate of $\xi$ for dual-axis swallowing accelerometry signals can be computationally costly. Hence, some approximation is needed. Before processing further, let us consider the available information. The location and duration (i.e., onset and offset) of swallows are only approximately known. In addition, it is known that $\boldsymbol{\phi}$ contains data that are sampled either from $g_1(\boldsymbol{\phi}|\theta_1)$ or $g_2(\boldsymbol{\phi}|\theta_2)$, depending on whether or not a swallow occurred. Therefore, rather than solving (13), only indicator functions defined as

$$u_{g_1}(\phi_i) = \begin{cases} \kappa, & \phi_i \sim g_1(\boldsymbol{\phi}\,|\theta_1) \\ 0, & \text{otherwise} \end{cases} \tag{14}$$

$$u_{g_2}(\phi_i) = \begin{cases} 1 - \kappa, & \phi_i \sim g_2(\boldsymbol{\phi}\,|\theta_2) \\ 0, & \text{otherwise} \end{cases} \tag{15}$$

can be formed, where $0 \leq \kappa \leq 1$. It is clear that $u_{g_1} + u_{g_2} = 1$. The functions introduced by (14) and (15) indicate the presence of different segments (i.e., no swallow or swallow), but the functions do not reveal any information about the time boundaries of these segments. Therefore, the next step is to determine these boundaries. Let us write the two indicator functions as a matrix $U = [u_{g_1}\ u_{g_2}]$. Furthermore, the segment space is the set

$$S_\phi = \left\{ U \in V_U \,|u_{g_1}, u_{g_2} \in [0,1]\,; u_{g_1} + u_{g_2} = 1; \right.$$
$$\left. 0 < \sum_{i=1}^{N} u_{g_{ji}} < N \quad \text{for } j = 1,2 \right\} \tag{16}$$

where $u_{g_{ji}} = u_{g_j}(\phi_i)$ and $V_U$ is the vector space of $U$. To find these segments, i.e., the regions representing when $\phi$ was sampled from either distribution, an objective function $J_m(U, \mathbf{v}) : S_\phi \times \mathbb{R}^+$ should be minimized [25]

$$J_m\,(U, \mathbf{v}) = \sum_{i=1}^{N} \sum_{j=1}^{2} \left(u_{g_{ji}}\right)^m (d_{ji})^2 \tag{17}$$

where

$$(d_{ji})^2 = \|\boldsymbol{\phi}_i - v_j\|^2 \tag{18}$$

is the inner product induced norm; $v_j$ is the prototype of $u_{g_j}$, $j = 1, 2$; and $m$ is the weighting exponent given by $m \in [1, \infty)$. In this paper, $m = 2$. However, it should be noted that $J_m(U, \mathbf{v})$ can be minimized only if $d_{ji} > 0$ for $\{j, i | 1 \leq j \leq 2, 1 \leq i \leq N\}, m > 1$, and $u_{g_j}$, $v_j$ are obtained through the following iterative steps:

$$u_{g_{jk}} = \left[ \sum_{o=1}^{2} \left( \frac{d_{jk}}{d_{ok}} \right)^{2/(m-1)} \right]^{-1} \tag{19}$$

$$v_j = \frac{\sum_{k=1}^{N} \left(u_{g_{jk}}\right)^m \boldsymbol{\phi}_k}{\sum_{k=1}^{N} \left(u_{g_{jk}}\right)^m}, \qquad \text{for } j = 1, 2. \tag{20}$$

This formulation is a two-class fuzzy c-means optimization problem. For complete proof of the previous statements, refer to [25]. Furthermore, this minimization can be simply realized through Picard iteration of (19) and (20) [25].

1) Randomly initialize $U^{(0)} \in S_\phi$, and then at steps $h = 1, 2, \ldots$.
2) Calculate $\{\mathbf{v}_j^{(h)}\}$ with (20) and $U^{(h-1)}$.
3) Compute $U^{(h)}$ using $\{\mathbf{v}_j^{(h)}\}$ and (19).
4) If $\|U^{(h)} - U^{(h-1)}\| \leq \epsilon$, stop; otherwise, increment $h$ and return to step 2.

These steps yield two indicator functions, $u_{g_1}$ and $u_{g_2}$, which denote the absence or presence of swallowing on one axis. For the dual-axis recordings, there are four indicator functions: $u_{g_1\mathrm{AP}}$, $u_{g_2\mathrm{AP}}$, $u_{g_1\mathrm{SI}}$, and $u_{g_2\mathrm{SI}}$, with $u_{g_2\mathrm{AP}}$ and $u_{g_2\mathrm{SI}}$ representing independently the absence or presence of swallowing vibrations in the A-P and S-I directions, respectively. However, excessive noise along one of the axes may lead to an incorrect estimate of swallow multiplicity in the corresponding signal. Therefore, to obtain a more accurate estimate of the locations and durations of swallows, the indicator functions from both axes should be multiplied. Therefore, the dual-axis indicator function $u_{\mathrm{DA}}$ is given by

$$u_{\mathrm{DA}} = u_{g_2\mathrm{AP}} \times u_{g_2\mathrm{SI}} = \begin{cases} \rho, & \phi \sim g_2(\phi\,|\theta_2) \\ 0, & \text{otherwise} \end{cases} \tag{21}$$

where $0 \ll \rho \leq 1$. If desired, $u_{\mathrm{DA}}$ can be turned into a binary indicator sequence as

$$u_{\mathrm{DA}} = \begin{cases} 1, & \rho \geq \gamma \\ 0, & \text{otherwise} \end{cases} \tag{22}$$

where $\gamma$ is a predetermined threshold value. The proposed modification of Wang and Willett's algorithm is intended to make the algorithm applicable to very long and noisy datasets.

### C. Algorithm Evaluation

The accuracy of the proposed segmentation algorithm was studied in two ways: first, using a set of simulated test signals with known change points, i.e., swallow locations, and second, using a subset of signals with 295 real swallows manually extracted by two SLPs. In the analysis of both synthetic and real signals, the values used for $L_{\min}$ and $L_{\max}$ are 2500 and 40 000 points, respectively. Furthermore, $\gamma = 0.05$ is used for the synthetic signals, while $\gamma = 0.1$ is used for the real signals.

*1) Validation With Synthetic Test Signals:* In the collected data, exact locations of swallow onsets and offsets were unknown as corresponding videofluoroscopic sequences were not acquired. The synthetic signals with known change points thus provided a gold standard against which the segmentation algorithm could be benchmarked.

To ensure that the test signals mimicked the dual-axis swallowing accelerometry signals acquired in this experiment, the following data generation rules applied.

1) For every realization, two signals should be generated: one simulating acceleration in the A-P direction and the other simulating acceleration in S-I direction.
2) There should be five distinct intervals where the variance of the signals increases above the baseline variance.
3) Each of the five intervals should have random duration and random frequency components to mimic intersubject variations.

The following definition of a signal $s_j(n)$ adheres to the previous rules

$$s_j(n) = \begin{cases} s_o(n) + \sum_{w=1}^{4} 0.2 \sin(2\pi f_{jw} nT), & n_1 \leq n \leq n_2 \\ s_o(n) + \sum_{w=1}^{4} 0.2 \sin(2\pi f_{jw} nT), & n_3 \leq n \leq n_4 \\ s_o(n) + \sum_{w=1}^{4} 0.2 \sin(2\pi f_{jw} nT), & n_5 \leq n \leq n_6 \\ s_o(n) + \sum_{w=1}^{4} 0.2 \sin(2\pi f_{jw} nT), & n_7 \leq n \leq n_8 \\ s_o(n) + \sum_{w=1}^{4} 0.2 \sin(2\pi f_{jw} nT), & n_9 \leq n \leq n_{10} \\ s_o(n), & \text{otherwise} \end{cases} \tag{23}$$

with

$$s_o(n) = \sum_{l=1}^{15} b_{jl} \sin(2\pi f_{jl} nT + \theta_l) \tag{24}$$

and where $j = 1, 2$ indexes the two directions; $T = 0.0001$ s; $1 \leq n \leq N$ and $N \sim \mathcal{N}(60\,0000, (50\,000)^2)$ with a constraint that $N > 150\,000$; $N > n_{10} > n_9 > \cdots > n_1$; $|n_{2q} - n_{2q-1}| \sim \mathcal{N}(250\,000, (5000)^2)$ for $1 \leq q \leq 5$ with a constraint that $|n_{2q} - n_q| > 5000$; $n_{2\kappa+1} - n_{2\kappa-1} = \lfloor N/5 \rfloor$, where $1 \leq \kappa \leq 4$; $b_{jl}$ is uniformly drawn from $[0, 0.05]$; $f_{jl}$ is uniformly drawn from $[1, 5000]$; $\theta_l$ is uniformly drawn from $[0, \pi]$; and $f_{jw} \sim \mathcal{N}(90, (15)^2)$ with a constraint that $f_{jw} > 1$. Using the earlier definition, 1000 pairs of dual-axis test signals were simulated. The top graph of Fig. 2 depicts a typical simulated test signal.

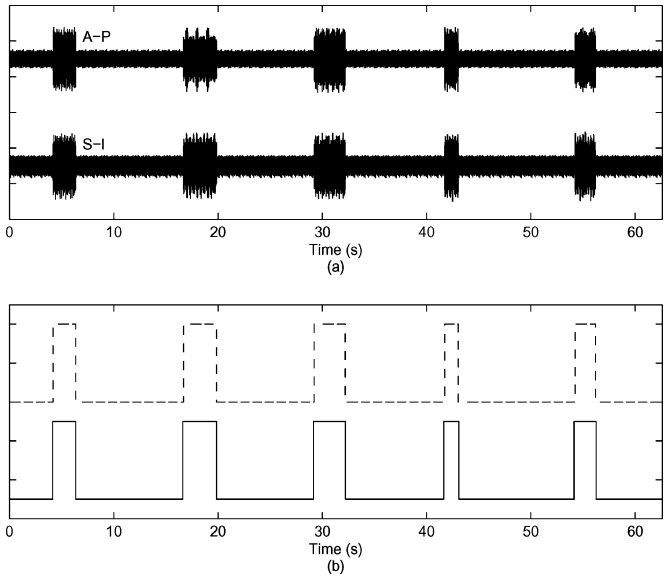


Fig. 2. Segmentation of test signals. (a) Realization of the simulated signal. (b) Actual indicator sequence (dashed line) and the indicator sequence produced by the algorithm (solid line).

Accuracy was defined as the number of correctly identified high-variance segments divided by the number of all high-variance segments. To be considered correct, an extracted segment had to overlap with the corresponding known segment by at least 90%.

It should be noted that the model for dual-axis swallowing accelerometry signals given by (23) does not necessarily represent realistic swallowing signals, since the physiological characteristics of such signals are still largely unknown. The proposed model rather depicts statistical behavior of these signals, i.e., the activity regions have higher variances than the baseline regions, and is only used for an accuracy analysis of the proposed segmentation algorithm.

*2) Validation Against Manually Segmented Swallows:* As a second evaluation step, two SLPs manually segmented 19 recordings representing saliva swallows (dry swallows), 20 recordings representing water swallows (wet swallows), and 19 recordings representing water swallows in the chin tuck position (wet chin tuck). Manual segmentation involved the location of onsets and offsets by visual inspection and auditory verification. Each recording contained five or six swallows, yielding a total of 295 swallows. It should be noted that the selected recordings were chosen to fairly represent the different age and gender groups of the population under study.

In the validation against the human expert, we defined a correctly segmented swallow as one in which there was a minimum 90% overlap with the SLP extracted swallow. A sample swallowing accelerometry signal is depicted in Fig. 3(a) along with a binary indicator function, where "high" denotes the presence of a

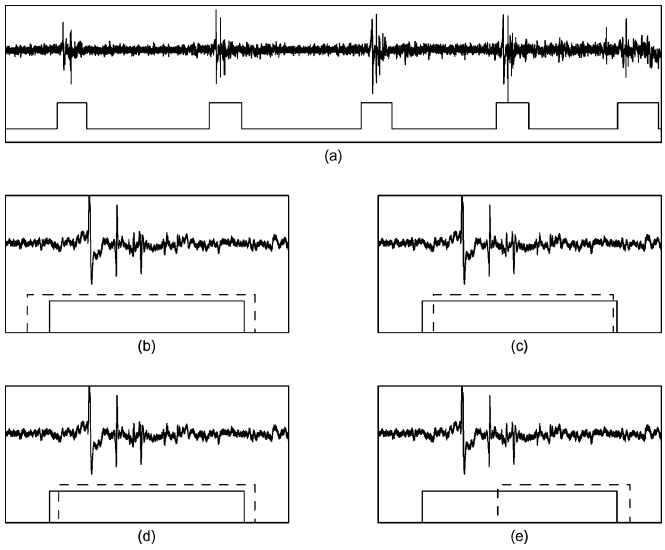


Fig. 3. Definition of a correctly segmented swallow. (a) Signal (top) and a binary function (bottom) indicating the occurrence of swallows as pinpointed by an SLP. (b)–(d) Correctly segmented swallows where the algorithm (pulse with dashed line) slightly over- or underestimates the swallow duration extracted by the SLP (pulse with solid line). (e) Incorrectly segmented swallow.

swallow as indicated by the SLP. The second swallow is arbitrarily selected in Fig. 3(b)–(e) to illustrate different segmentation possibilities. In each graph, the dashed lines represent possible indicator functions obtained by the algorithm. Evidently, to be considered a correctly segmented swallow as in Fig. 3(b)–(d), most of the swallow duration ($\geq 90\%$) as indicated by the SLP must be captured. Otherwise, the algorithm is deemed to have incorrectly identified the swallow, as exemplified in Fig. 3(e).

After signals from all 408 participants had been segmented, we used nonparametric inferential statistical methods and linear regression analysis to test for potential effects of gender, BMI, and age on swallowing duration.

## IV. Results and Discussion

### A. Segmentation of Synthetic Test Signals

With the 1000 pairs of simulated test signals, the extraction accuracy of the proposed algorithm was $97.7 \pm 1.3\%$. Also, the average duration of the extracted segment was $(2.59 \pm 0.50) \times 10^4$ points, which is statistically similar ($p = 0.18$) to the average duration of the original segments ($2.5 \times 10^4$ points). This close agreement between original and extracted segment onsets, offsets, and durations is illustrated in the bottom graph of Fig. 2. Results with the test signals demonstrate that the proposed algorithm is indeed capable of accurately extracting segments with elevated variance and varying length from long time series.

### B. Segmentation of Real Swallowing Signals

The results of the validation against manual segmentation by the SLPs are summarized in Table I. Each row in the table represents the performance of the segmentation algorithm on one type of swallow.

TABLE I
ACCURACY OF PROPOSED SEGMENTATION ALGORITHM FOR SUBSET OF SWALLOWS MANUALLY SEGMENTED BY SLP

| Swallowing Type | TNS | CSS | %CSS | Duration (sec) | |
|---|---|---|---|---|---|
| | | | | SLP | Algorithm |
| Dry swallows | 98 | 98 | 100 | $2.4 \pm 1.2$ | $2.3 \pm 1.4$ |
| Wet swallows | 102 | 98 | 96.1 | $1.7 \pm 0.6$ | $2.0 \pm 0.7$ |
| Wet chin tuck | 95 | 83 | 87.4 | $1.9 \pm 0.6$ | $3.1 \pm 1.0$ |
| Overall | 295 | 279 | 94.6 | $2.0 \pm 0.9$ | $2.4 \pm 1.1$ |

TNS: total number of swallows; CSS: number of correctly segmented swallows; and % CSS: percentage of correctly segmented swallows.

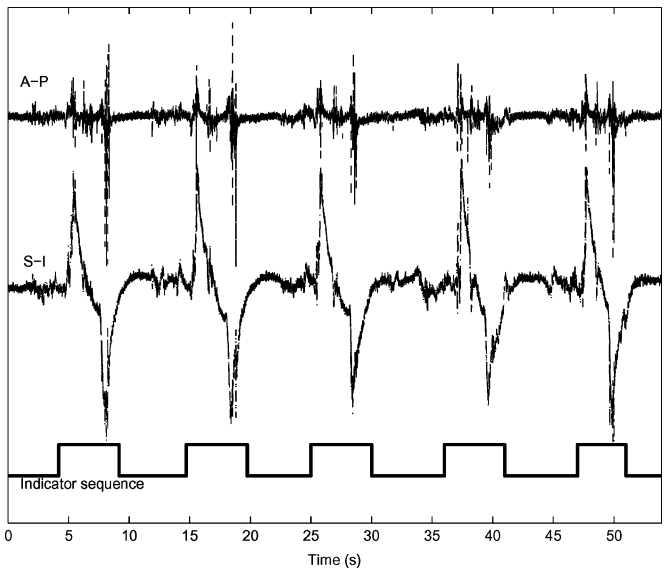


Fig. 4. Sample of wet chin tuck swallowing vibrations in A-P and S-I directions along with the indicator sequence obtained by the proposed algorithm.

TABLE II
DURATION OF SWALLOWING SEGMENTS GROUPED BY GENDER (408 PARTICIPANTS)

| Swallowing Type | All participants | Male | Female |
|---|---|---|---|
| Dry swallows* | $2.9 \pm 1.2$ | $3.1 \pm 1.3$ | $2.8 \pm 1.2$ |
| Wet swallows* | $2.3 \pm 0.7$ | $2.5 \pm 0.8$ | $2.2 \pm 0.6$ |
| Wet chin tuck | $3.7 \pm 1.4$ | $3.8 \pm 1.4$ | $3.6 \pm 1.4$ |
| Overall* | $2.9 \pm 1.2$ | $3.0 \pm 1.3$ | $2.8 \pm 1.2$ |

An asterisk denotes a statistically significant gender difference.

Evidently, the proposed algorithm achieves very good overall accuracy considering that the segmentation is performed on raw data (i.e., there was no preprocessing of data). The lowest accuracy is achieved for wet chin tuck swallows. However, this is expected since the wet chin tuck swallows are manifested through very complex signals, especially in the S-I direction, as shown in Fig. 4. These vibrations are caused by head movement and, in some cases, can overwhelm the vibrations of interest in the A-P direction, encumbering detection by the proposed algorithm.

So far, extraction accuracy has been discussed. The temporal accuracy of the algorithm should be examined as well. To this end, a comparison of the durations of manually and automatically segmented swallows was carried out. The average durations are shown in the last two columns of Table I. Several observations are in order. While the durations for dry and wet swallows appear to agree closely with the durations obtained by the SLP, a Wilcoxon rank-sum test revealed that the durations

TABLE III
DURATION OF SWALLOWING SIGNALS GROUPED BY BMI (408 PARTICIPANTS)

| Swallowing Type | $BMI < 18.5$ underweight | $18.5 \leq BMI < 25$ normal | $25 \leq BMI < 30$ overweight | $BMI \geq 30$ obese |
|---|---|---|---|---|
| Dry swallows | $2.7 \pm 1.2$ | $2.9 \pm 1.3$ | $2.9 \pm 1.2$ | $3.0 \pm 1.3$ |
| Wet swallows | $2.3 \pm 0.6$ | $2.3 \pm 0.7$ | $2.3 \pm 0.7$ | $2.3 \pm 0.6$ |
| Wet chin tuck* | $3.3 \pm 0.9$ | $3.4 \pm 1.3$ | $3.9 \pm 1.5$ | $4.0 \pm 1.3$ |
| Overall* | $2.7 \pm 0.9$ | $2.8 \pm 1.2$ | $3.0 \pm 1.3$ | $3.0 \pm 1.3$ |

An asterisk indicates significant dependence of duration on BMI ($p$=0.05).

are statistically similar only for the dry swallows ($p = 0.10$). The durations of the wet chin tuck swallows were overestimated by the algorithm, on average, by 1 s. This overestimation was due to the overwhelming motion artifact depicted in Fig. 4. With additional measurements, e.g., a head motion sensor, these swallow durations could be further refined. We further note that the segmented vibration signals likely included events associated with both the oral and pharyngeal phases of swallowing, each of which persists for approximately 1 s [26]. This would explain the algorithm's overall average duration of $2.4 \pm 1.1$ s in Table I, which, incidentally, is consistent with the temporal characterization of the oral–pharyngeal phase of swallowing reported by Sonies *et al.* [19].

### C. Analysis of Swallowing Signals' Duration

The second goal of this study was to uncover any associations between the duration of the segmented signals and the anthropometric/demographic variables, namely, gender, BMI, or age. The results of such an analysis are summarized in Tables II–IV and are obtained using all 9800 swallows. The table entries are average durations of the segmented signals in seconds for different levels of the selected variables (gender, BMI, or age). While both neck circumference and BMI were measured, a simple linear regression analysis showed that these variables were highly correlated. Therefore, neck circumference was discarded and BMI was chosen for further analysis. The latter variable is appealing since participants can be grouped according to standardized BMI intervals [27].

In Table II, we see that events associated with wet swallows are consistently manifested as the shortest signals (Wilcoxon rank-sum test, $p \ll 10^{-5}$), while the events associated with wet chin tuck swallows tend to embody the longest signals (Wilcoxon rank-sum test, $p \ll 10^{-5}$). The extended length of the wet chin tuck swallows has already been attributed to the algorithm's overestimation in the presence of excessive motion artifact. Regarding the other types of swallows, Sonies *et al.* also found that wet swallows were shorter than dry ones [19]. Finally, the swallowing signals obtained from male participants were longer than those extracted from female participants for dry and wet swallow types (Wilcoxon rank-sum test, $p \ll 10^{-5}$). This difference in duration can be attributed to gender-based anatomical differences in the oropharyngeal mechanism [28]. The gender difference did not appear in the wet chin tuck swallows due to the inflated variability in durations for this task, likely due to motion artifact.

Inspection of Table III suggests that as a person's BMI increases, the duration of the swallowing events increases as well. According to a regression test, this dependence on BMI is statistically significant for the events associated with wet chin tuck swallows ($p \ll 10^{-5}$). A possible explanation is that an increase in adipose tissue results in an attenuation of the signal amplitude and velocity [29]. The latter effect may allow the vibration signal to decay more slowly, thereby extending the duration of the measured activity.

TABLE IV
DURATION OF SWALLOWING SIGNALS GROUPED BY AGE (408 PARTICIPANTS)

| Swallowing Type | $Age \leq 30$ | $31 \leq Age \leq 45$ | $46 \leq Age \leq 60$ | $Age \geq 61$ |
|---|---|---|---|---|
| Dry swallows* | $2.7 \pm 1.1$ | $2.9 \pm 1.2$ | $3.0 \pm 1.2$ | $3.2 \pm 1.5$ |
| Wet swallows* | $2.2 \pm 0.6$ | $2.3 \pm 0.8$ | $2.3 \pm 0.7$ | $2.5 \pm 0.6$ |
| Wet chin tuck* | $3.5 \pm 1.2$ | $3.5 \pm 1.4$ | $4.0 \pm 1.5$ | $3.8 \pm 1.5$ |
| Overall* | $2.7 \pm 1.1$ | $2.9 \pm 1.2$ | $3.0 \pm 1.3$ | $3.1 \pm 1.4$ |

An asterisk indicates significant dependence of duration on age ($p$=0.05).

We further remark that as the age of the participant increases, the duration of the events associated with a swallow tends to increase as well (Table IV). Based on the results of a regression test, this dependence on age is statistically significant for the events associated with all types of swallows ($p \ll 10^{-5}$). This trend may be attributed to the age-related decoupling of oral and pharyngeal stages of swallowing [26], leading to longer overall swallowing times.

As the last remark, it should be pointed out that the current data collection has been carried out in a relatively controlled environment, i.e., healthy subjects with no known swallowing difficulties and good cognitive skills. Hence, excellent segmentation accuracy has been achieved without any preprocessing of the data. Nevertheless, as has been pointed out in Section II, recordings containing disturbance signals have not been used in the current study. Disturbance signals such as cough, speech, and excessive head movements confound the proposed segmentation algorithm. However, data from a pathological population would likely be plagued with such artifacts. Therefore, prior to applying the proposed algorithm to patient data, we anticipate that it would be necessary to explicitly remove disturbance signals from the dual-axis swallowing accelerometry signals.

## V. CONCLUSION

In this paper, a sequential segmentation algorithm was proposed for dual-axis swallowing accelerometry signals, owing to their potential for noninvasive diagnosis of swallowing difficulties. The algorithm is based on a piecewise fuzzy partitioning of the signal and is well suited to long signals with nonstationary variance. Dual-axis swallowing accelerometry signals from three swallowing tasks completed by 408 healthy participants were automatically segmented. In comparison with simulated signals with known swallowing locations and a subset of real swallows extracted manually by an SLP, the proposed algorithm yielded over 90% accuracy. Of the three types of swallows considered, wet chin tuck swallows were the least accurately

segmented due to excessive motion artifacts. Durations of the extracted segments increased with increasing BMI (wet chin tuck type) and age ($p = 0.05$), while male participants exhibited longer swallowing events than females for dry and wet swallows ($p = 0.05$).

## REFERENCES


[1] N. P. Reddy, E. P. Canilang, R. C. Grotz, M. B. Rane, J. Casterline, and B. R. Costarella, "Biomechanical quantification for assessment and diagnosis of dysphagia," *IEEE Eng. Med. Biol. Mag.*, vol. 7, no. 3, pp. 16–20, Sep. 1988.

[2] N. P. Reddy, B. R. Costarella, R. C. Grotz, and E. P. Canilang, "Biomechanical measurements to characterize the oral phase of dysphagia," *IEEE Trans. Biomed. Eng.*, vol. 37, no. 4, pp. 392–397, Apr. 1990.

[3] N. P. Reddy, E. P. Canilang, J. Casterline, M. B. Rane, A. M. Joshi, R. Thomas, and R. Candadai, "Noninvasive acceleration measurements to characterize the pharyngeal phase of swallowing," *J. Biomed. Eng.*, vol. 13, pp. 379–383, Sep. 1991.

[4] N. R. Reddy, A. Katakam, V. Gupta, R. Unnikrishnan, J. Narayanan, and E. P. Canilang, "Measurements of acceleration during videofluorographic evaluation of dysphagic patients," *Med. Eng. Phys.*, vol. 22, no. 6, pp. 405–412, Jul. 2000.

[5] A. Das, N. P. Reddy, and J. Narayanan, "Hybrid fuzzy logic committee neural networks for recognition of swallow acceleration signals," *Comput. Methods Prog. Biomed.*, vol. 64, no. 2, pp. 87–99, Feb. 2001.

[6] J. Lee, S. Blain, M. Casas, D. Kenny, G. Berall, and T. Chau. (2006, Jul.). A radial basis classifier for the automatic detection of aspiration in children with dysphagia. *J. Neuroeng. Rehabil.*, [Online]. *3*, p. 17. Available: http://www.jneuroengrehab.com/content/3/1/14/abstract

[7] S. Suryanarayanana, N. P. Reddy, and E. P. Canilang, "A fuzzy logic diagnosis system for classification of pharyngeal dysphagia," *Int. J. Biomed. Comput.*, vol. 38, no. 3, pp. 207–215, Mar. 1995.

[8] T. Chau, D. Chau, M. Casas, G. Berall, and D. J. Kenny, "Investigating the stationarity of paediatric aspiration signals," *IEEE Trans. Neural Syst. Rehabil. Eng.*, vol. 13, no. 1, pp. 99–105, Mar. 2005.

[9] H. Liang, L. Sakari, and H. Iiro, "A heart sound segmentation algorithm using wavelet decomposition and reconstruction," in *Proc. 19th Annu. Int. Conf. IEEE Eng. Med. Biol. Soc.*, vol. 4, Chicago, IL, Oct. 30–Nov. 2, 1997, pp. 1630–1633.

[10] S. S. Park and N. S. Kim, "On using multiple models for automatic speech segmentation," *IEEE Trans. Audio, Speech Lang. Process.*, vol. 15, no. 8, pp. 2202–2212, Nov. 2007.

[11] T. Lan, D. Erdogmus, M. Pavel, and S. Mathan, "Automatic frequency bands segmentation using statistical similarity for power spectrum density based brain computer interfaces," in *Proc. Int. Joint Conf. Neural Netw. (IJCNN 2006)*, Vancouver, BC, Canada, Jul. 16–21, pp. 4650–4655.

[12] S. Krishnan, R. M. Rangayyan, G. D. Bell, C. B. Frank, and K. O. Ladly, "Adaptive filtering, modelling and classification of knee joint vibroarthrographic signals for non-invasive diagnosis of articular cartilage pathology," *Med. Biol. Eng. Comput.*, vol. 35, no. 6, pp. 677–684, Nov. 1997.

[13] P. S. L. Rosa, A. Nehorai, H. Eswaran, C. L. Lowery, and H. Preissl, "Detection of uterine MMG contractions using a multiple change point estimator and the $k$-means cluster algorithm," *IEEE Trans. Biomed. Eng.*, vol. 55, no. 2, pp. 453–467, Feb. 2008.

[14] R. J. Lehner and R. M. Rangayyan, "A three-channel microcomputer system for segmentation and characterization of the phonocardiogram," *IEEE Trans. Biomed. Eng.*, vol. BME-34, no. 6, pp. 485–489, Jun. 1987.

[15] H. L. Chan, C. H. Lin, and Y. L. Ko, "Segmentation of heart rate variability in different physical activities," in *Proc. 2003 Comput. Cardiol. Conf.*, Thessaloniki, Greece, Sep. 21–24, pp. 97–100.

[16] Y. Kim and G. H. McCullough, "Maximum hyoid displacement in normal swallowing," *Dysphagia*, vol. 23, no. 3, pp. 274–279, 2007.

[17] R. Ishida, J. B. Palmer, and K. M. Hiiemae, "Hyoid motion during swallowing: Factors affecting forward and upward displacement," *Dysphagia*, vol. 17, no. 4, pp. 262–272, Dec. 2002.

[18] J. A. Y. Cichero and B. E. Murdoch, "The physiologic cause of swallowing sounds: Answers from heart sounds and vocal tract acoustics," *Dysphagia*, vol. 13, no. 1, pp. 39–52, Jan. 1998.

[19] B. C. Sonies, L. J. Parent, K. Morrish, and B. J. Baum, "Durational aspects of the oral–pharyngeal phase of swallow in normal adults," *Dysphagia*, vol. 3, no. 1, pp. 1–10, Mar. 1988.

[20] J. W. Bennett and C. M. Steele, "An examination of normal sip size behaviour in a natural drinking condition versus instructed experimental conditions," *Dysphagia*, vol. 22, no. 4, p. 387, Oct. 2007.

[21] R. Andre-Obrecht, "A new statistical approach for the automatic segmentation of continuous speech signals," *IEEE Trans. Acoust., Speech, Signal Process.*, vol. 36, no. 1, pp. 29–40, Jan. 1988.

[22] M. Lavielle, "Optimal segmentation of random processes," *IEEE Trans. Signal Process.*, vol. 46, no. 5, pp. 1365–1373, May 1998.

[23] R. J. Kenefic, "An algorithm to partition DFT data into sections of constant variance," *IEEE Trans. Aerosp. Electron. Syst.*, vol. 34, no. 3, pp. 789–795, Jul. 1998.

[24] Z. Wang and P. Willett, "Two algorithms to segment white Gaussian data with piecewise constant variances," *IEEE Trans. Signal Process.*, vol. 51, no. 2, pp. 373–385, Feb. 2003.

[25] J. C. Bezdek, *Pattern Recognition Wth Fuzzy Objective Function Algorithms*. New York: Plenum, 1981.

[26] J. F. Tracy, J. A. Logemann, P. J. Kahrilas, P. Jacob, M. Kobara, and C. Krugler, "Preliminary observations on the effects of age on oropharyngeal deglutition," *Dysphagia*, vol. 4, no. 2, pp. 90–94, Jun. 1989.

[27] World Health Organization. (2008, Mar. 3). Global database on body mass index [Online]. Available: http://www.who.int/bmi/index.jsp

[28] J. A. Y. Cichero and B. E. Murdoch, "Acoustic signature of the normal swallow: Characterization by age, gender, and bolus volume," *Ann. Otol., Rhinol. Laryngol.*, vol. 111, no. 7, pp. 623–632, Jul. 2002.

[29] F. A. Duck, *Physical Properties of Tissue: A Comprehensive Reference Book*. London, U.K.: Academic, 1990.


**Ervin Sejdić** (S'00–M'08) received the B.E.Sc. and Ph.D. degrees in electrical engineering from the University of Western Ontario, London, ON, Canada, in 2002 and 2007, respectively.

He is currently with the Bloorview Research Institute and the Institute of Biomaterials and Biomedical Engineering, University of Toronto, Toronto, ON. He was engaged in the field of wireless communications and also focused on signal processing. His current research interests include biomedical signal processing, time–frequency analysis, signal processing for wireless communications, and compressive sensing.

Dr. Sejdić won prestigious research scholarships from the Natural Sciences and Engineering Research Council of Canada in 2003 and 2005.

**Catriona M. Steele** received the B.A. (Hons.) degree in psychology and German, the M.H.Sc. degree in speech language pathology, and the Ph.D. degree in speech language pathology and neuroscience from the University of Toronto, Toronto, ON, Canada, in 1988, 1991, and 2003, respectively.

She was a practicing Speech Language Pathologist at Baycrest and St. Joseph's Health Centre, Toronto. She is currently a Senior Scientist at the Toronto Rehabilitation Institute, University of Toronto, where she is also an Associate Professor in the Department of Speech-Language Pathology. Her current research interests include swallowing physiology and rehabilitation.

Dr. Steele received the Canadian Institutes of Health Research New Investigator Award in Aging and an Early Researcher Award from the Ontario Ministry of Research and Innovation.

**Tom Chau** (S'93–M'98–SM'03) received the B.A.Sc. degree in engineering science and the M.A.Sc. degree in electrical and computer engineering from the University of Toronto, Toronto, ON, Canada, in 1992 and 1994, respectively, and the Ph.D. degree in systems design engineering from the University of Waterloo, Waterloo, ON, in 1997.

He was with IBM Canada. He is currently a Senior Scientist at the Bloorview Kids Rehab, Toronto, where he is also an Associate Professor, Graduate Coordinator of the Clinical Engineering Program at the Institute of Biomaterials and Biomedical Engineering, and a Canada Research Chair in Pediatric Rehabilitation Engineering. His current research interests include the development and investigation of intelligent technologies and analytical techniques to decode functional intention of individuals with disabilities.